Supplementary Material for

Readily Prepared, Inclusion Forming Chiral Calixsalens

A. Janiak,* M. Petryk, L. J. Barbour,* M. Kwit*

Data Page Number

Experimental details

^{1}H and ^{13}C NMR spectra were recorded on Varian VNMR-S 400 MHz instrument. Chemical shifts (δ) are reported in ppm relative to $SiMe_4$ and coupling constants (*J*) are given in Hz. Mass spectra were run on a MaldiSYNAPT G2-S HDMS. UV and ECD spectra were recorded in spectroscopic grade dichloromethane using a JASCO J-810 instrument. FTIR spectra were measured on a Bruker FT-IR IFS 66/s in KBr pellets. A PerkinElmer 341 polarimeter was used for optical rotation ($[\alpha]_D$) measurements (ca. 20 °C). Flash column chromatography was performed on Merck Kieselgel type 60 (250 - 400 mesh). Merck Kieselgel type $60F_{254}$ analytical plates were employed for TLC. Melting points were measured on Büchi Melting Point B-545 and uncorrected.

All known compounds were identified by spectroscopic comparison with authentic samples.

Aldehydes **2a**, **2c**-**2g** were prepared according to the literature procedures.[1-4]

5-Fluoro-2-hydroxyisophthaldehyde (**2b**) was prepared similarly to the procedure previously described:[3]

4-Fluorophenol (3.83 g, 34.2 mmol) and hexamethylenetetramine (9.60 g, 68.5 mmol) were dissolved in anhydrous TFA (60 mL) under argon atmosphere and the resulting yellow solution was refluxed for 24 hours (color change to deep orange). The mixture was poured into 4 M HCl (200 mL) and stirred for 60 min, after which it was extracted with CH_2Cl_2 (3 × 100 mL). The combined organic extracts were washed with 4 M HCl (2 × 100 mL) and brine (3 × 100 mL), then dried over Na_2SO_4 and evaporated to give a yellow crystalline residue. The product was purified by chromatography on silica gel, using CH_2Cl_2 as eluent. This gave **2b** as yellow solid sufficiently pure for further reactions; yield: 2.78 g (48%).

^{1}H NMR ($CDCl_3$): δ = 11.45 (s, 1H, -OH), 10.21 (s, 2H, -CHO), 7.95 (s, 2H, Ar-H).

General procedure for synthesis of calixsalens 3a-3g:

To a 0.5 M solution of (*R*,*R*)-1,2-diaminocyclohexane (**1**, 228 mg, 2 mmol) in dry dichloromethane (4 mL) an equimolar solution of appropriate aldehyde **2** (2 mmol) in 4 mL of dry dichloromethane was added drop wise. Then the whole mixture was stirred under argon atmosphere for 24 hours at room temperature. After evaporation of all volatiles (the temperature of water bath did not exceed 25 °C) the crude product was dried under high vacuum for 5 hours at room temperature and crystallized.

The crystals suitable for X-ray analyses were obtained as follow: the dry crude material was dissolved in dry dichloromethane (0.5 M solution) and put in a bottle in open vial. Another open vial filled with dry diethyl ether was put into the same bottle then the bottle was closed tightly. Depending on the structure of macrocycle, crystallization took place from 4 days up to three weeks. Calixsalens **3f** and **3g** were crystallized by slow evaporation of dichloromethane from dichloromethane-methanol solution of respective macrocycle.

Calixsalens **3a**, **3c**-**3f** gave all spectra identical as these previously published.[5-7]

Calixsalen **3b**, yield 86% after crystallization from dichloromethane-diethyl ether; m.p. > 300 °C (decomp.); $[\alpha]_D^{20}$=260 (*c*=0.5 in dichloromethane); ^{1}H NMR (400 MHz, $CDCl_3$, 20 °C, TMS): δ=13.82 13.82 (s, 1H), 8.63 (d, *J* = 2.4 Hz, 1H), 8.19 (s, 1H), 7.54 (dd, *J* = 9.2, 3.2 Hz, 1H), 6.87 (dd, *J* = 7.9, 3.2 Hz, 1H), 3.53 – 3.14 (m, 2H), 2.07 – 1.03 (m, 8H); ^{13}C NMR (75 MHz, $CDCl_3$, 20 °C, TMS): δ=162.54, 162.51, 157.38, 156.07, 154.82, 154.80, 153.73, 124.69, 124.63, 119.26, 119.19, 119.03, 115.69, 115.46, 65.81, 33.23, 33.00, 24.26, 24.16, 15.24; IR (KBr): 3433, 1639, 1592 cm^{-1}; HR MS (MALDI TOF): *m*/*z*: 739.3574 [M+H^+], calcd. for $C_{42}H_{46}F_3N_6O_3$=739.3583.

Calixsalen **3g**, yield 52% after crystallization from dichloromethane-methanol; m.p. > 300 °C (decomp.); $[\alpha]_D^{20}$=3 (*c*=0.5 in dichloromethane); ^{1}H NMR (400 MHz, $CDCl_3$, 20 °C, TMS): δ=14.22 (s, 1H), 8.66 (s, 1H), 7.97 (s, 1H), 7.76 (d, *J* = 2.6 Hz, 1H), 7.16-7.08 (m, 15H); 7.02 (d, *J* = 2.5 Hz, 1H), 3.31-3.20 (m, 2H), 1.73-1.25 (m, 8H); ^{13}C NMR (75 MHz, $CDCl_3$, 20 °C, TMS): δ=163.42, 160.16, 154.88, 146.70, 135.90, 135.13, 132.48, 131.04, 127.04, 125.79, 123.28, 118.42, 64.19, 33.55, 24.29; IR (KBr): 3433, 1633, 1591 cm^{-1}; HR MS (MALDI TOF): *m*/*z*: 1411.7130 [M+H^+], calcd. for $C_{99}H_{91}F_3N_6O_3$=1411.7153.

Calculation details

Starting geometries of monomeric macrocycles **3a**-**3e** with assumed conformations were obtained from crystallographic data and pre-optimized at the M06L/6-31G(d) level.[8] The structures of respective monomers were further optimised in vacuo and in dichloromethane solution, using the polarizable continuum model (IEFPCM)[9] all with the use of M06L functional in conjunction with 6-311G(d,p) basis set. The structures thus obtained were the real minimum energy conformers (no imaginary frequencies have been found). The same scheme was used in the cases of respective dimeric structures of **3a**-**3e**. Additionally, for all investigated compounds ECD spectra were measured in dichloromethane solution and calculated at the IEFPCM/TDDFT/6-311G(d,p) level for all stable geometries, including monomers and dimers, according to the procedure previously described.[10] We employed four different hybrid functionals to calculate ECD spectra: M06-2X,[8] B2LYP,[11] LC-wPBE [12] and CAM-B3LYP.[13] Rotatory strengths were calculated using both length and velocity representations. In the present study, the differences between the length and velocity calculated values of rotatory strengths were quite small and for this reason only the velocity representations were further used. The ECD spectra were simulated by overlapping Gaussian functions [14] for each transition, according to the procedure previously described.[10] All calculations were performed with the use of Gaussian 09 package.[15] It worth to note that all of employed functionals produced similar

results, thus in the main text we restrict discussion to the results obtained with the use of M06-2X hybrid functional only.

In the case of calixsalen **3e** rotation of methoxyl groups has only negligible effect on the calculated ECD spectra thus only the most stable conformer of **3e** is discussed.

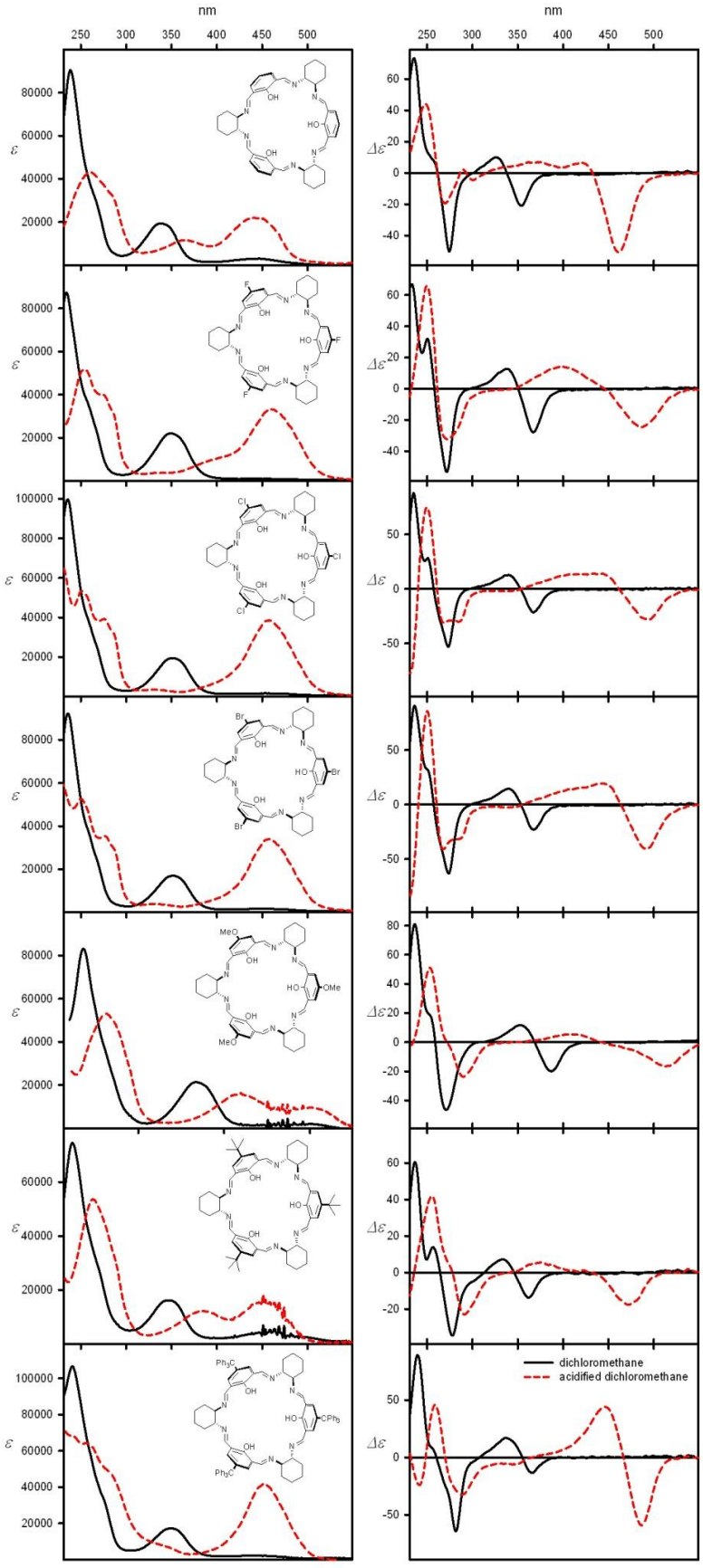

Figure S1. UV (left column) and ECD (right column) spectra of calixsalens **3a**-**3f** measured in dichloromethane (black solid lines) and in acidified dichloromethane (red dashed lines).

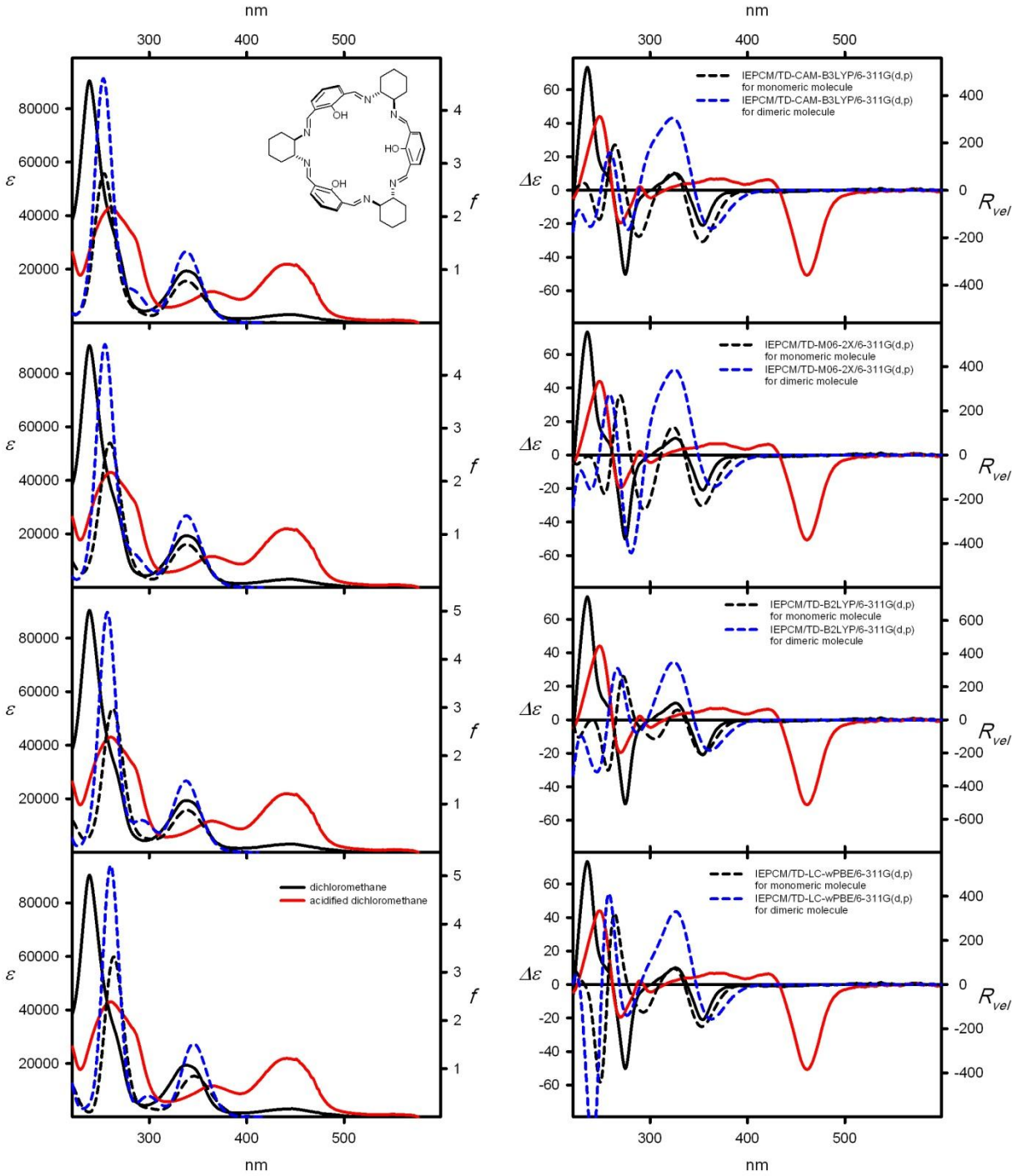

Figure S2. UV (left column) and ECD (right column) spectra of calixsalen **3a** measured in dichloromethane (black solid lines) and in acidified dichloromethane (red lines) and calculated at various levels of theory for monomeric (black dashed lines) and dimeric (blue dashed lines) structures optimized at the IEFPCM/M06L/6-311G(d,p) level. All calculated spectra were wavelength corrected to match experimental long-wavelength UV maximum.

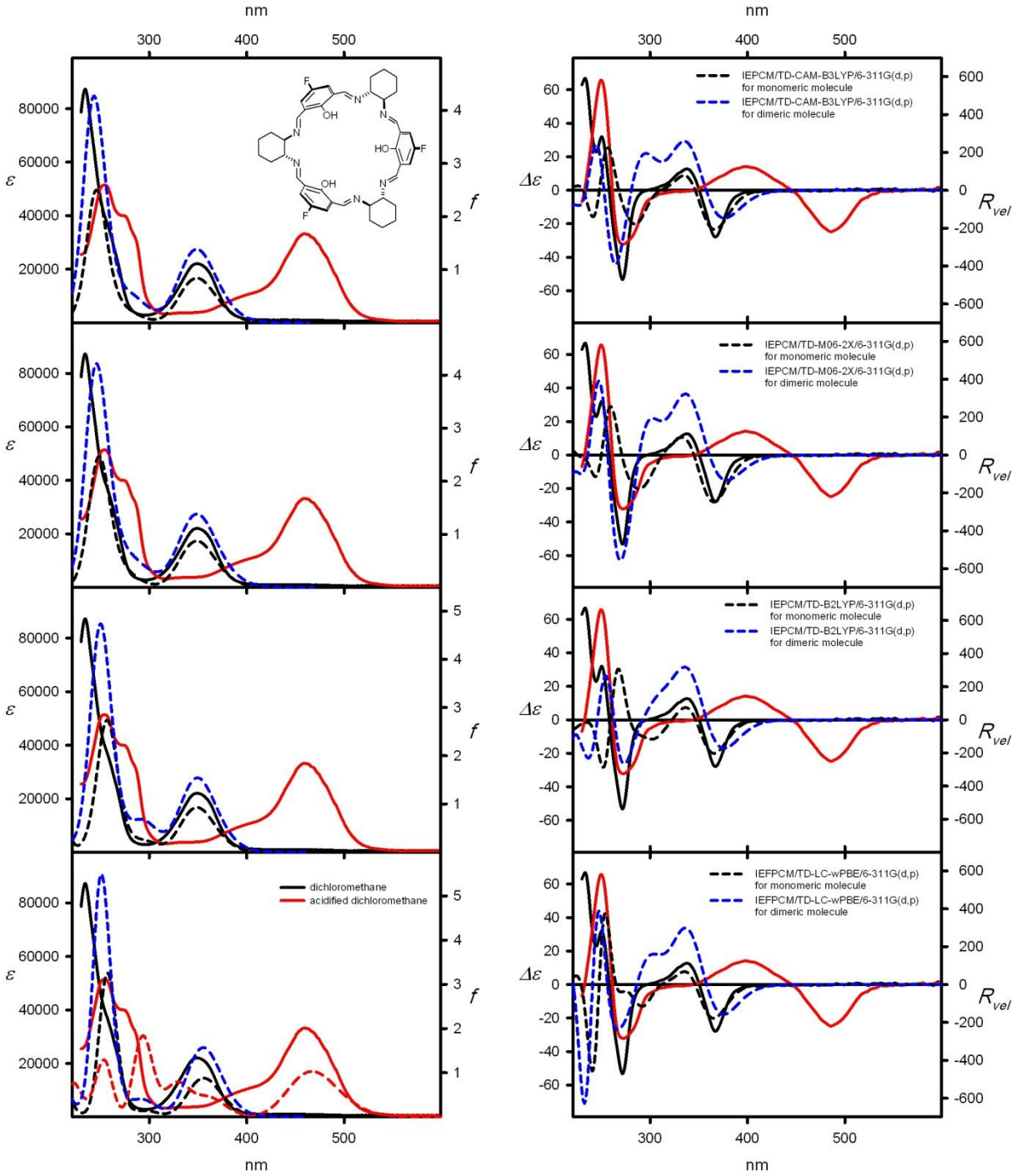

Figure S3. UV (left column) and ECD (right column) spectra of calixsalen **3b** measured in dichloromethane (black solid lines) and in acidified dichloromethane (red lines) and calculated at various levels of theory for monomeric (black dashed lines) and dimeric (blue dashed lines) structures optimized at the IEFPCM/M06L/6-311G(d,p) level. All calculated spectra were wavelength corrected to match experimental long-wavelength UV maximum.

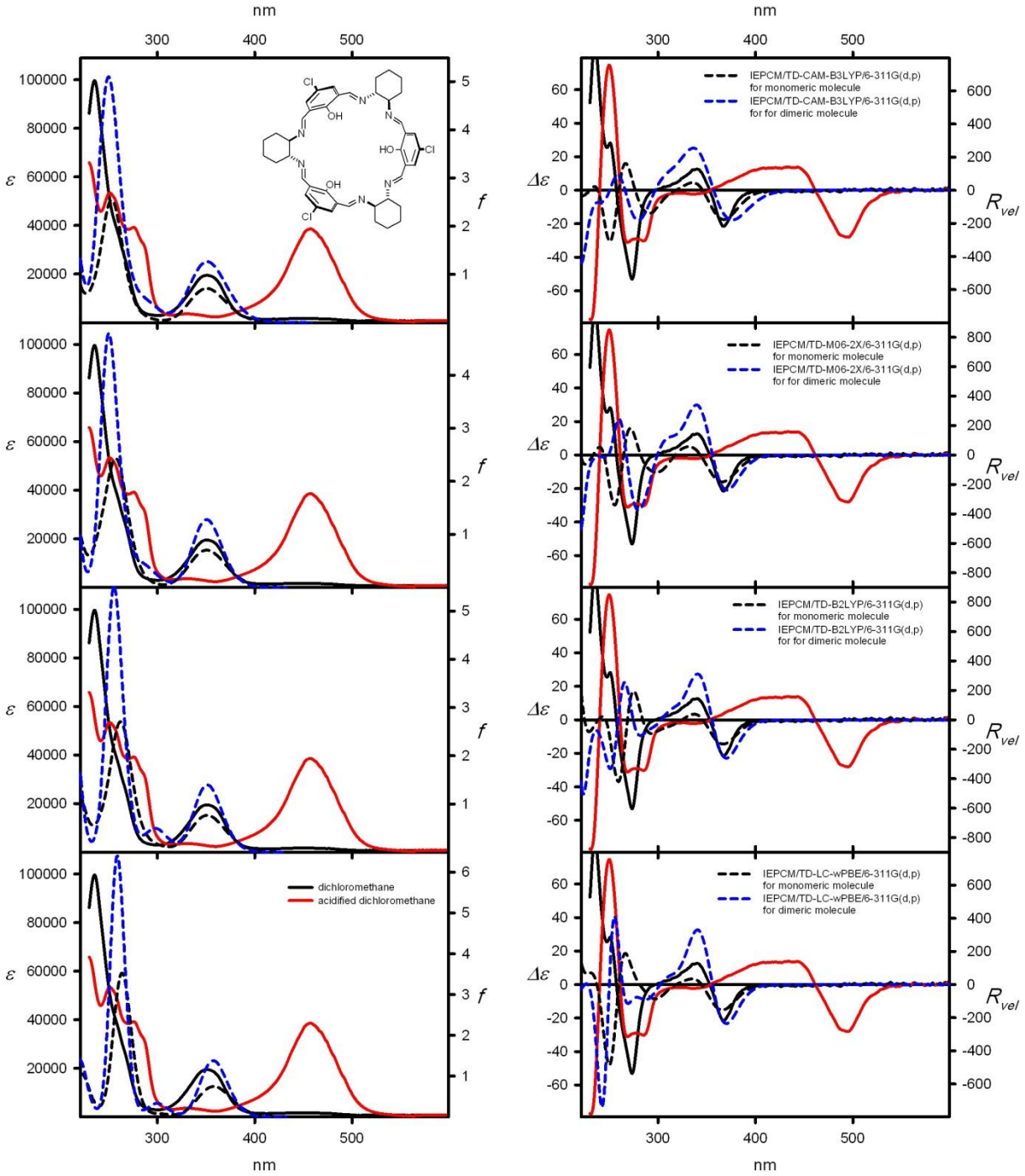

Figure S4. UV (left column) and ECD (right column) spectra of calixsalen **3c** measured in dichloromethane (black solid lines) and in acidified dichloromethane (red lines) and calculated at various levels of theory for monomeric (black dashed lines) and dimeric (blue dashed lines) structures optimized at the IEFPCM/M06L/6-311G(d,p) level. All calculated spectra were wavelength corrected to match experimental long-wavelength UV maximum.

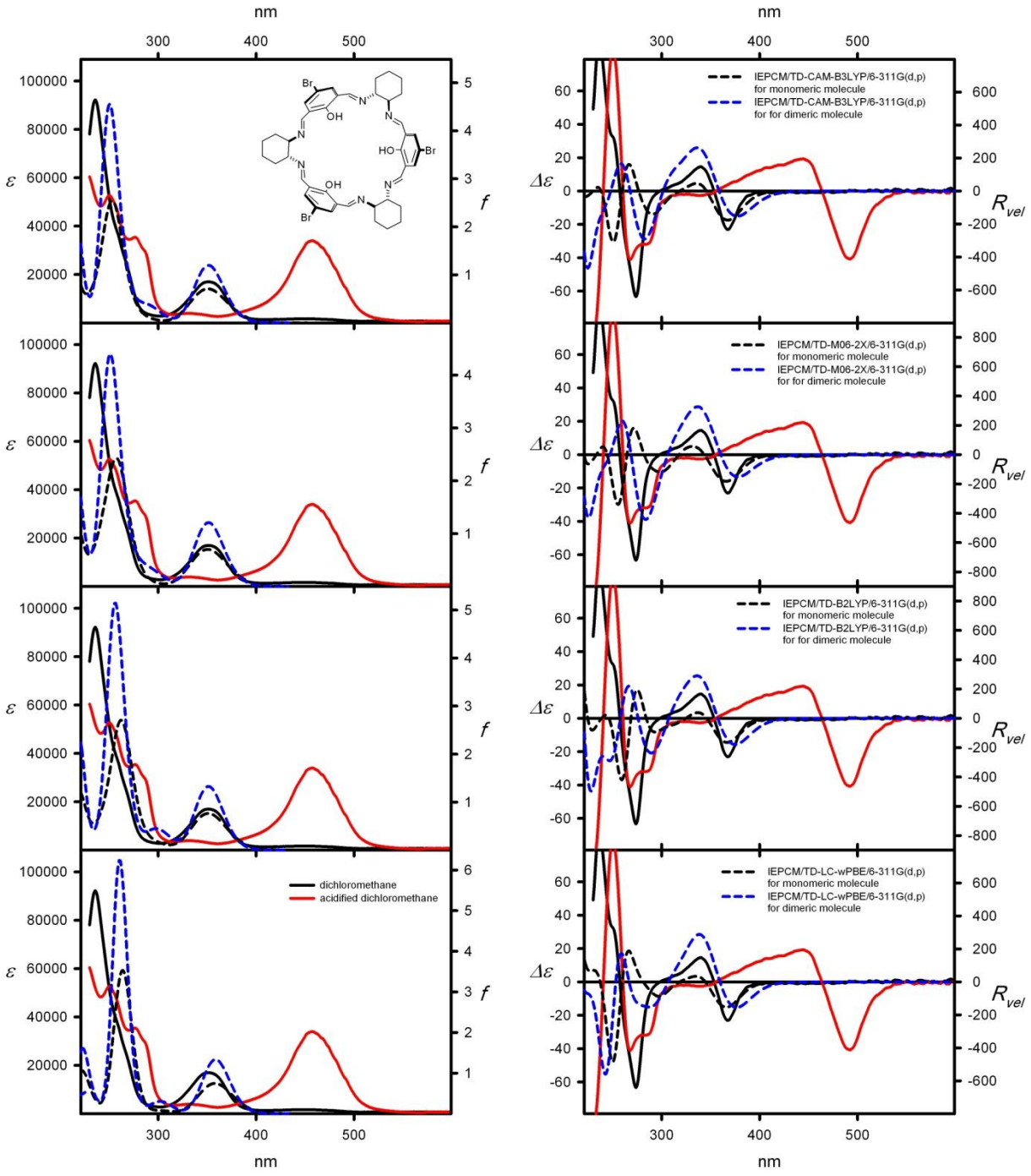

Figure S5. UV (left column) and ECD (right column) spectra of calixsalen **3d** measured in dichloromethane (black solid lines) and in acidified dichloromethane (red lines) and calculated at various levels of theory for monomeric (black dashed lines) and dimeric (blue dashed lines) structures optimized at the IEFPCM/M06L/6-311G(d,p) level. All calculated spectra were wavelength corrected to match experimental long-wavelength UV maximum.

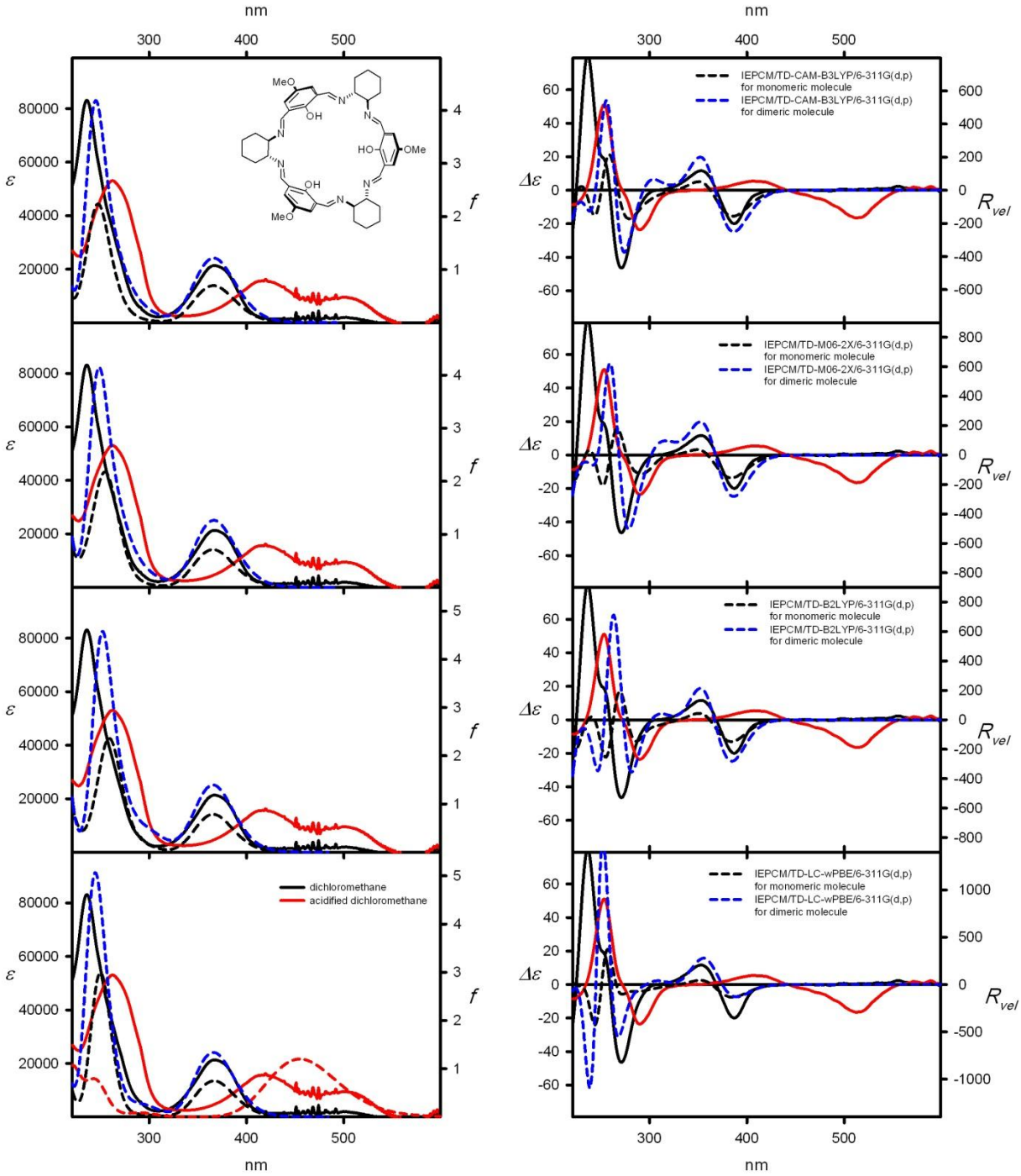

Figure S6. UV (left column) and ECD (right column) spectra of calixsalen **3e** measured in dichloromethane (black solid lines) and in acidified dichloromethane (red lines) and calculated at various levels of theory for monomeric (black dashed lines) and dimeric (blue dashed lines) structures optimized at the IEFPCM/M06L/6-311G(d,p) level. All calculated spectra were wavelength corrected to match experimental long-wavelength UV maximum.

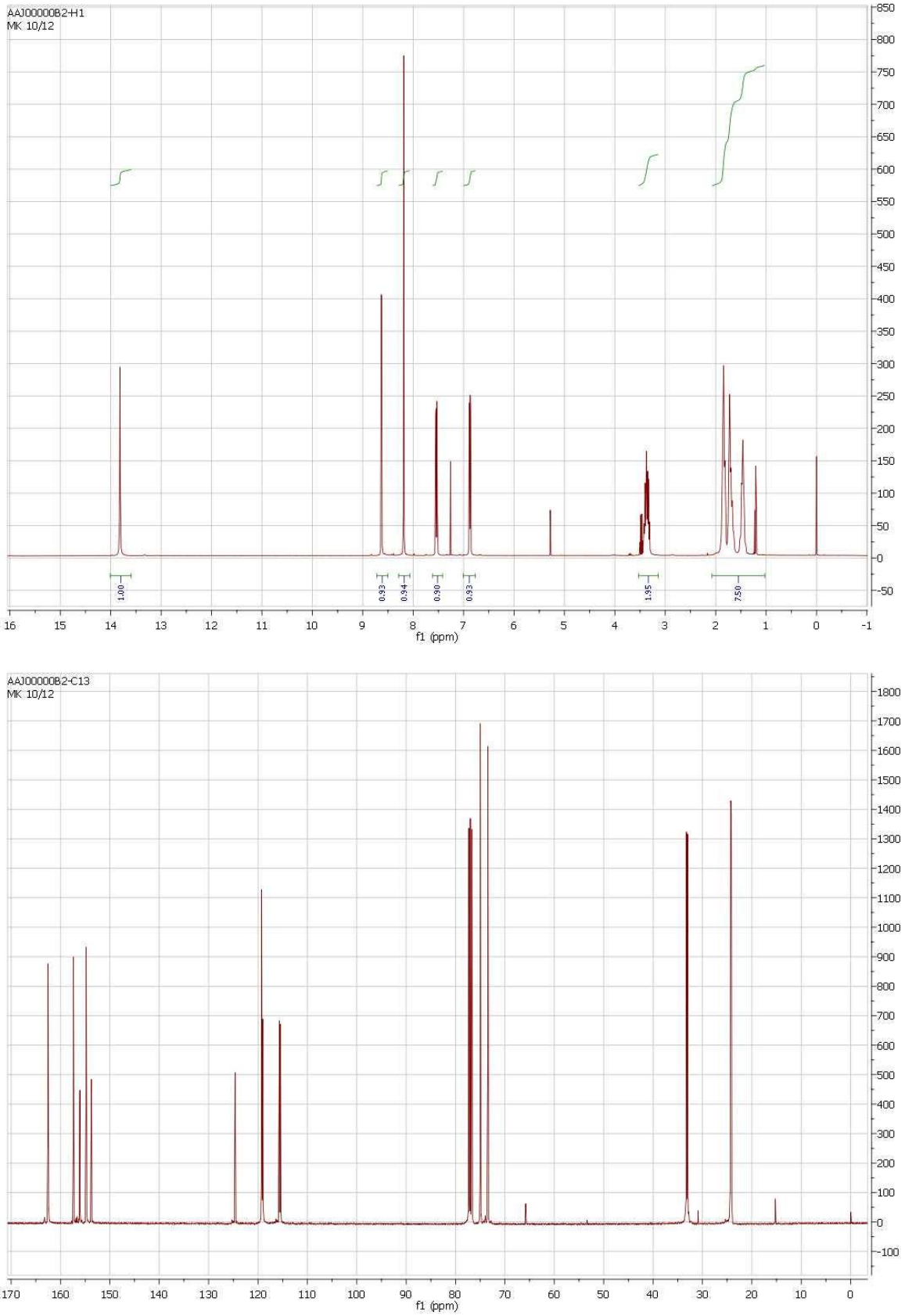

Figure S7. ^{1}H and ^{13}C NMR spectra of calixsalen **3b**.

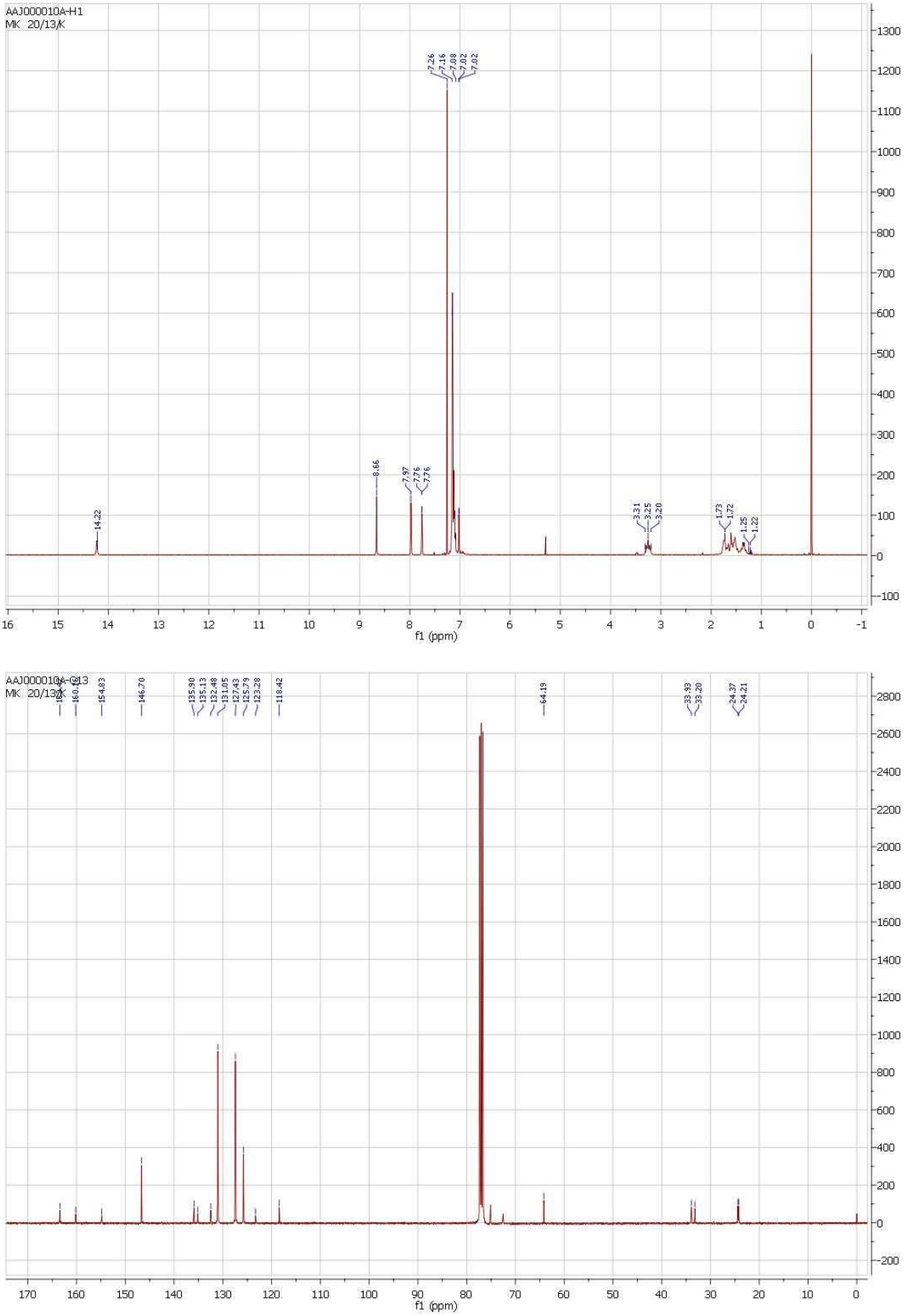

Figure S8. ^{1}H and ^{13}C NMR spectra of calixsalen **3g**.

Single-Crystal X-ray diffraction

Reflection intensities for **3a**, **3f$_{sCO2}$** and **3g$_{MeCN}$** were measured on a Bruker Quasar APEX DUO diffractometer using both Cu (λ=1.54178 Å) (**3g$_{MeCN}$**) and Mo microfocus source (λ=0.71073 Å) (**3a** & **3f$_{sCO2}$**). **3f** was measured on a Bruker SMART APEX equipped with MoKα radiation sealed tube source. Data reduction was carried out by means of a standard procedure using the Bruker software package SAINT.[16] The absorption correction was based on multiple and symmetry equivalent reflections in the data set by using the SADABS program.[17] Crystals of **3a** did not diffract above the resolution limit of 0.9 Å, this is why during data processing the resolution was restricted at the value of 0.9 Å. Hence the maximum sin(theta)/lambda for **3a** is below required limit of at least 0.6.

The diffraction measurements for the remaining crystals **3b-3e** and **3g** were carried out either on Agilent Technologies Xcalibur diffractometer (Eos detector) with graphite-monochromatized MoKα radiation (λ=0.71073 Å) (**3b** & **3c**) or SuperNova diffractometer equipped with a Cu microfocus source (λ=1.54178 Å) and 135 mm Atlas CCD (**3d**, **3e**, **3g**). Data reduction and analysis for these crystals were carried out with the CrysAlisPro program *v*.171.35.4.[18]

In all XRD experiments the temperature of the crystals was controlled with an Oxford Instruments Cryosystem cold nitrogen-gas blower. The structures were solved by direct methods using SHELXS97,[19] and refined by the full-matrix least-squares techniques with SHELXL97.[19] All heavy atoms were refined anisotropically. The hydrogen atoms bound to C atoms were placed at calculated positions and refined using a riding model, and their isotropic displacement parameters were given a value 20% higher than the isotropic equivalent for the atom to which the H atoms were attached (for methyl hydrogens this value has been increased to 50%). The positions of the hydroxyl H atoms firstly were located reliably on difference Fourier maps and then these H atoms were treated as riding with U_{iso}=1.2U_{iso}(O).

In **3g** the dichloromethane molecule located in the inner host cavity displays a disorder where the chlorine atoms as well as hydrogen atoms are split up into two positions while carbon atom is common. The occupancies of the two positions were refined to 0.79(2) and 0.21(2), respectively, summing up to the total occupancy of 1. Where necessary, the restraints for the 1,2- and 1,3-distances were applied.

In cases in which the value of the Flack parameter[20] was meaningless, the absolute structure of the investigated crystals was assumed from the known absolute configuration of the (*R*,*R*)-1,2-diaminecyclohexane which was used as a starting material in the syntheses. Graphical images were produced in Xseed[21] using Pov Ray[22] and with Mercury[23] programs.

Crystal data for 3a: $C_{42}H_{48}N_6O_3$, M_r=684.86, pale yellow plate, 0.40×0.35×0.07 mm^3, monoclinic, space group $P2_1$ (No. 4), a=14.489(8), b=16.788(10), c=15.691(9) Å, β=97.627(9)°, V=3783(4) Å^3, Z=4, D_c=1.203 g/cm^3, F_{000}=1464, Bruker Quasar APEX DUO, Mo Kα radiation, λ = 0.71073 Å, T = 120(2)K, $2\vartheta_{max}$ = 46.7°, 33895 reflections collected, 10962 unique (R_{int}=0.1734). Final *GooF*=0.963, *R1*=0.0674, *wR2*=0.1246, *R* indices based on 5885 reflections with I>2sigma(I) (refinement on F^2), 925 parameters, 1 restraint. Lp and absorption corrections applied, μ=0.077 mm^{-1}. Absolute structure parameter=3(2) (Flack, H. D. *Acta Cryst*. **1983**, *A39*, 876-881).

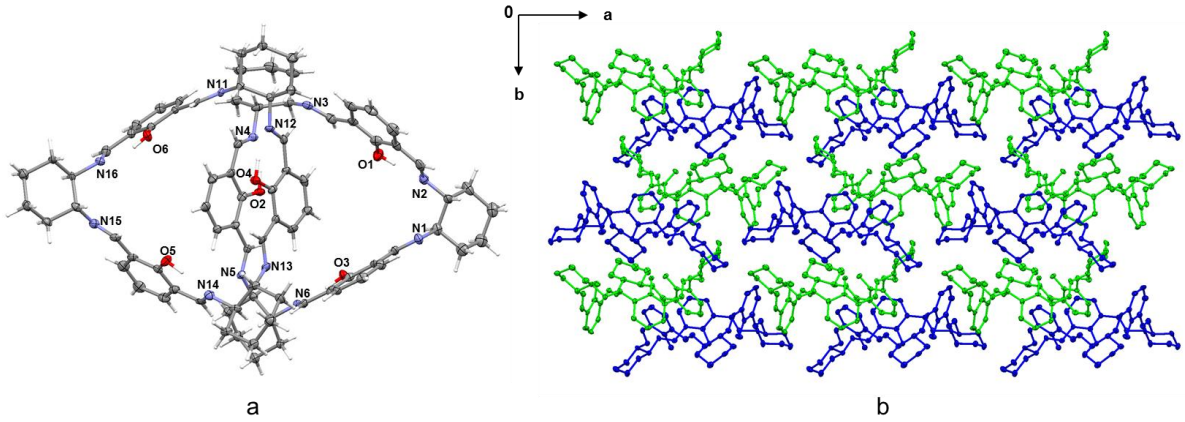

a b

Figure S9. a) An illustration of asymmetric unit of **3a**. For clarity only the heteroatoms were labeled. Ellipsoids are drawn at the 40% probability level, hydrogen atoms are represented by spheres of arbitrary radii. b) A packing diagram of **3a** as viewed along the *c* lattice direction. The two symmetry independent host molecules which form a dimer are shown in green and blue in ellipsoid style. All H atoms are omitted for clarity.

Crystal data for 3b: $C_{42}H_{45}F_3N_6O_3$, M_r=738.84, light yellow block, 0.60×0.28×0.15 mm^3, monoclinic, space group $P2_1$ (No. 4), a=14.6367(4), b=17.6967(4), c=15.0640(4) Å, β=94.450(2)°, V=3890.13(17) Å^3, Z=4, D_c=1.262 g/cm^3, F_{000}=1560, Xcalibur, Eos detector, MoKα radiation, λ=0.71073 Å, T=120(1)K, $2\theta_{max}$=57.6°, 31842 reflections collected, 17092 unique (R_{int}=0.0317). Final *GooF*=1.043, *R1*=0.0524, *wR2*=0.1087, *R* indices based on 12811 reflections with I>2sigma(I) (refinement on F^2), 973 parameters, 1 restraint. Lp and absorption corrections applied, μ=0.091 mm^{-1}. Absolute structure parameter=-0.1(5) (Flack, H. D. *Acta Cryst*. **1983**, *A39*, 876-881).

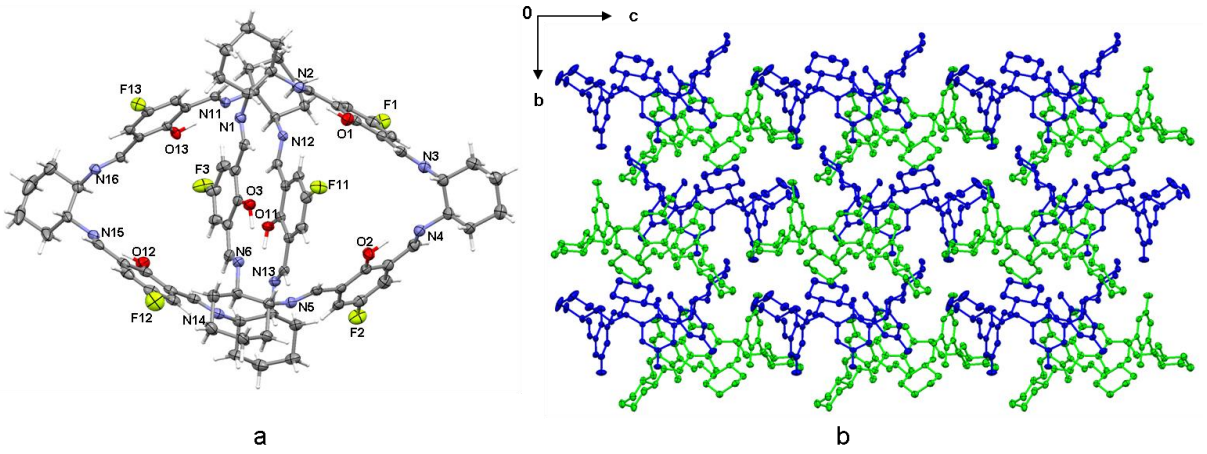

Figure S10. a) An illustration of asymmetric unit of **3b**. For clarity only the heteroatoms were labeled. Ellipsoids are drawn at the 40% probability level, hydrogen atoms are represented by spheres of arbitrary radii. b) A packing diagram of **3b** as viewed along the *a* lattice direction. The two symmetry independent host molecules which form a dimer are shown in green and blue in ellipsoid style. All H atoms are omitted for clarity.

Crystal data for 3c: $C_{42}H_{45}Cl_3N_6O_3$, M_r=788.19, light yellow plate, 0.50×0.24×0.08 mm^3, monoclinic, space group $P2_1$ (No. 4), a=14.6060(4), b=18.7364(5), c=14.7922(4) Å, β=92.420(2)°, V=4044.48(19) Å^3, Z=4, D_c=1.294 g/cm^3, F_{000}=1656, Xcalibur, Eos detector, MoKα radiation, λ=0.71073 Å, T=130(1)K, $2\theta_{max}$=57.5°, 45026 reflections collected, 18081 unique (R_{int}=0.0382). Final *GooF*=0.994, *R1*=0.0490, *wR2*=0.0997, *R* indices based on 14047 reflections with I>2sigma(I) (refinement on F^2), 997 parameters, 1 restraint. Lp and absorption corrections applied, μ=0.273 mm^{-1}. Absolute structure parameter= -0.04(3) (Flack, H. D. *Acta Cryst*. **1983**, *A39*, 876-881).

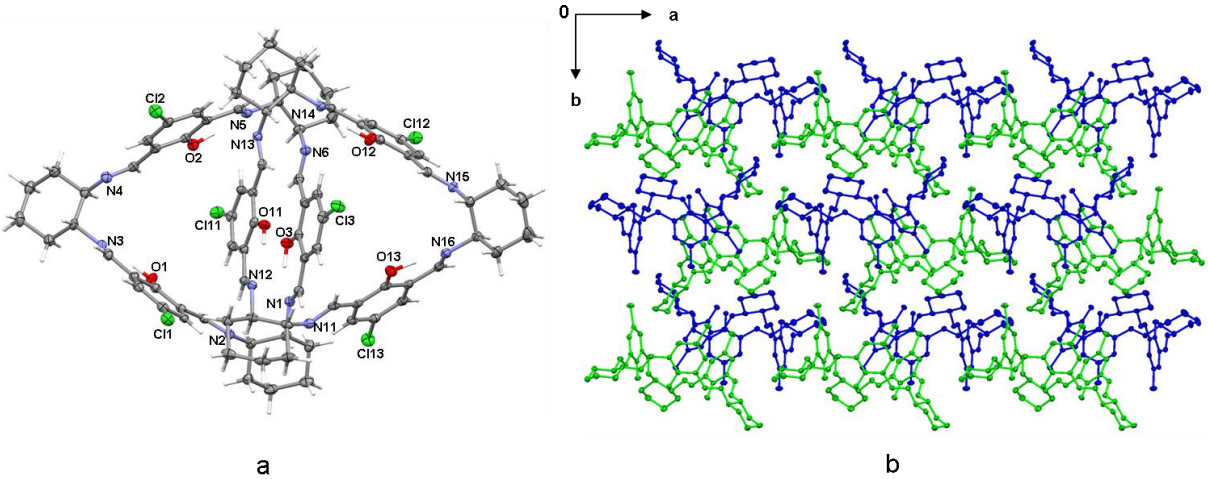

Figure S11. a) An illustration of asymmetric unit of **3c**. For clarity only the heteroatoms were labeled. Ellipsoids are drawn at the 40% probability level, hydrogen atoms are represented by spheres of arbitrary radii. b) A packing diagram of **3c** as viewed along the *c* lattice direction. The two symmetry independent host molecules which form a dimer are shown in green and blue in ellipsoid style. All H atoms are omitted for clarity.

Crystal data for 3d: $C_{42}H_{45}Br_3N_6O_3$, M_r=921.57, yellow block, 0.26×0.18×0.10 mm^3, monoclinic, space group $P2_1$ (No. 4), a=14.5208(2), b=19.0262(3), c=14.9678(2) Å, β=91.8320(10)°, V=4133.13(10) Å^3, Z=4, D_c=1.481 g/cm^3, F_{000}=1872, SuperNova, Atlas detector, CuKα radiation, λ=1.54178 Å, T=130(1)K, 2θ_{max}=153.1°, 61556 reflections collected, 17091 unique (R_{int}=0.0161). Final *GooF*=1.053, *R1*=0.0255, *wR2*=0.0672, *R* indices based on 17015 reflections with I>2sigma(I) (refinement on F^2), 973 parameters, 1 restraint. Lp and absorption corrections applied, μ=3.983 mm^{-1}. Absolute structure parameter= -0.015(7) (Flack, H. D. *Acta Cryst*. **1983**, *A39*, 876-881).

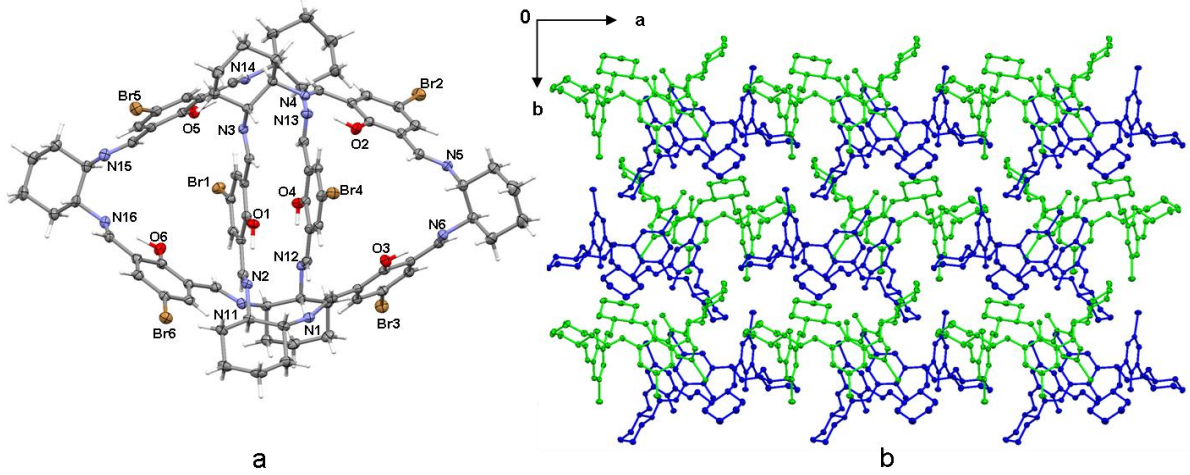

Figure S12. a) An illustration of asymmetric unit of **3d**. For clarity only the heteroatoms were labeled. Ellipsoids are drawn at the 40% probability level, hydrogen atoms are represented by spheres of arbitrary radii. b) A packing diagram of **3d** as viewed along the *c* lattice direction. The two symmetry independent host molecules which form a dimer are shown in green and blue in ellipsoid style. All H atoms are omitted for clarity.

Crystal data for 3e: 2($C_{45}H_{54}N_6O_6$)•$C_4H_{10}O$, M_r=1624.00, pale yellow needle, 0.50×0.06×0.06 mm^3, triclinic, space group $P1$ (No. 1), a=11.2310(3), b=16.5478(4), c=16.6580(4) Å, α=60.773(2), β=70.814(2), γ=73.664(2)°, V=2524.11(11) Å^3, Z=1, D_c=1.068 g/cm^3, F_{000}=870, SuperNova, Atlas detector, CuKα radiation, λ=1.54178 Å, T=130(2)K, 2θ_{max}=153.0º, 56259 reflections collected, 19930 unique (R_{int}=0.0299). Final *GooF*=1.058, *R1*=0.0540, *wR2*=0.1516, *R* indices based on 18377 reflections with I>2sigma(I) (refinement on F^2), 1080 parameters, 3 restraints. Lp and absorption corrections applied, μ=0.577 mm^{-1}. Absolute structure parameter=-0.08(12) (Flack, H. D. *Acta Cryst*. **1983**, *A39*, 876-881).

It was possible to only determine position for one solvent molecule in the crystal. The remaining solvent molecules were highly disordered and could not be resolved to yield a satisfactory model, therefore their unresolved electron density was treated with SQUEEZE as implemented in PLATON.[24] SQUEEZE analysis determined the number of electron count to be 137 ē in the accessible void volume of 445 Å^3 which is consistent with the void occuppied by 3 guest molecules (137/42 ~ 3). Since the crystals were obtained by the diffusion of diethyl ether in to a dichloromethane solution (both have 42 electrons) the squeezed electron count could define any combination of molecules of

both solvents that sums to 3. Taking into account the number of the squeezed molecules and solvent molecule that could be modelled, we established the ratio of host to guest as 1:2.

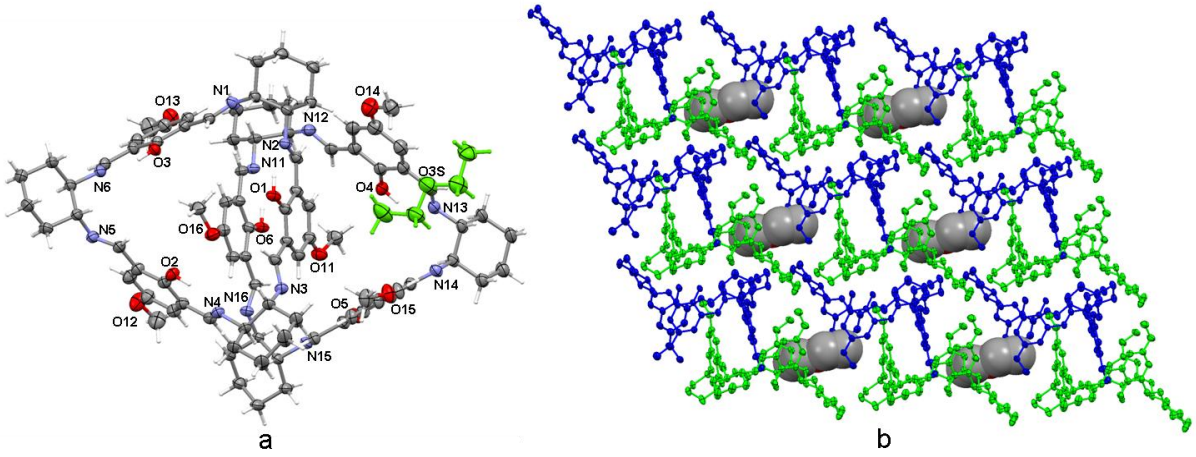

Figure S13. a) A perspective view of **3e**. For clarity only the heteroatoms were labeled. Ellipsoids are drawn at the 40% probability level, hydrogen atoms are represented by spheres of arbitrary radii. b) A packing diagram of **3e**. The two symmetry independent host molecules which form a dimer are shown in green and blue in ellipsoid style whereas guest molecules are shown as space-filling model. All H atoms are omitted for clarity.

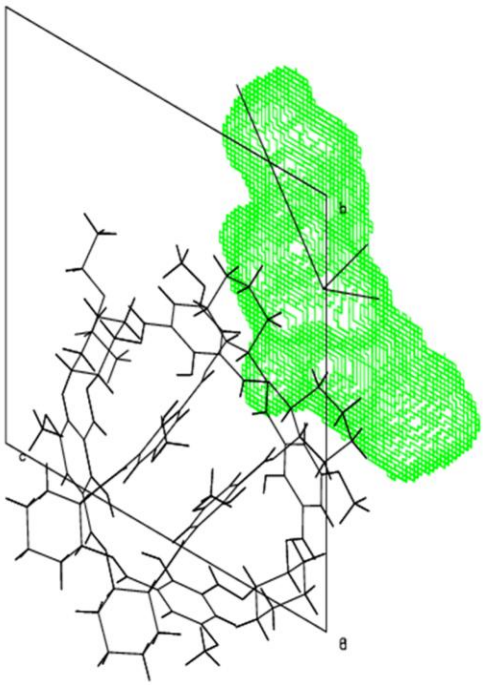

Figure S14. The diagram shows the void (in green) from which the solvent molecules were removed as viewed along *a* lattice direction.

Crystal data for 3f after squeezed: $C_{54}H_{72}N_6O_3$, M_r=853.18, yellow block, 0.55x0.40x0.25 mm^3, hexagonal, space group $P6_322$ (No. 182), a=b=18.740(3), c=22.056(3) Å, V=6708.3(17) $Å^3$, Z=4, D_c=0.845 g/cm^3, F_{000}=1848, MoKα radiation, λ=0.71073 Å, T=100(2)K, $2\vartheta_{max}$=51.3°, 36164 reflections collected, 4243 unique (R_{int}=0.0282). Final *GooF*=1.096, *R1*=0.0427, *wR2*=0.1151, *R* indices based on 3903 reflections with I>2sigma(I) (refinement on F^2), 193 parameters, 0 restraints. Lp and absorption corrections applied, μ=0.053 mm^{-1}. Absolute structure parameter=0.3(17) (Flack, H. D. *Acta Cryst*. **1983**, *A39*, 876-881).

In the crystal structure of **3f** solvent molecules are highly disordered and cannot be properly modelled therefore their contributions were removed from the diffraction data using the SQUEEZE. The estimated electron count is 283 in an accessible void volume of 2232.9 $Å^3$ and can indicate to squeezed of 16 molecules of methanol per unit cell (283/18~16). Taking into account the number of solvent molecules which were squeezed we determined host to guest ratio as 1:4

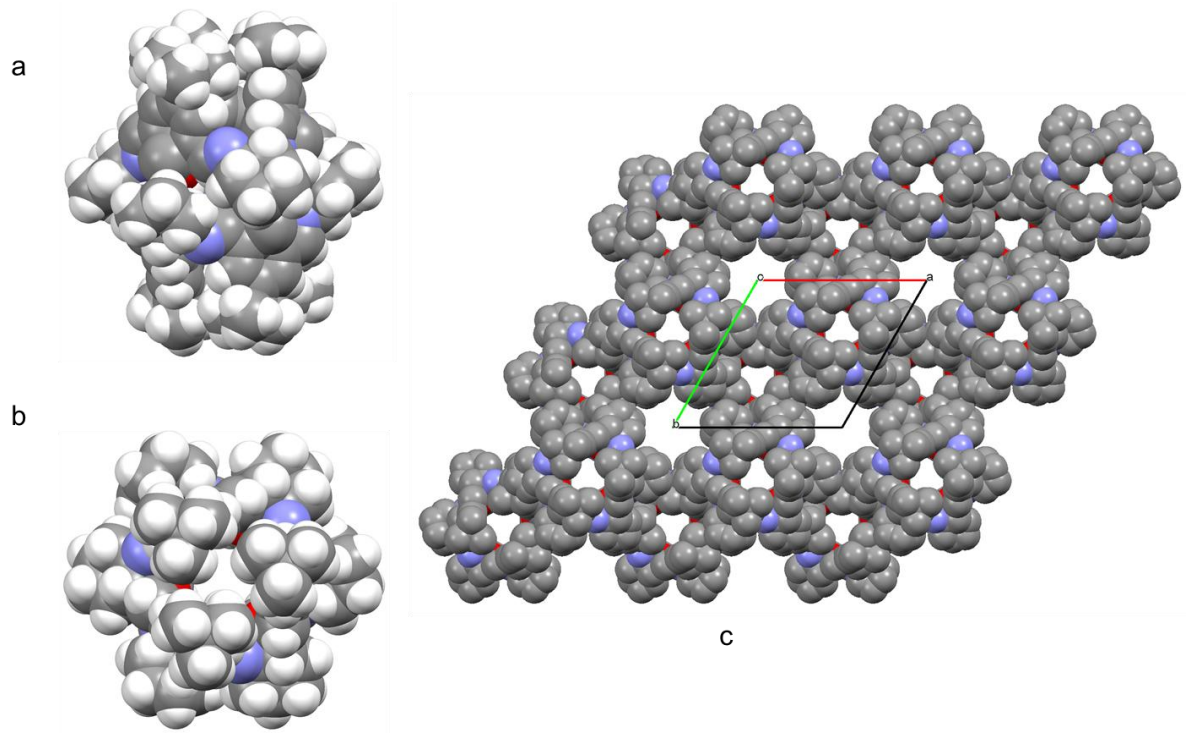

Figure S15. A side (a) and top (b) view of the capsule formed by two symmetry related calixsalen of **3f**. c) The host matrix of **3f** viewed along [001] shows two types of channels: narrow and wide, both able to accommodate solvent molecules. The narrow channels passes through the capsules (interior channels along 3-fold axis) while the wide channels are formed in the intramolecular space (exterior channels along 6_3 screw axis). Host molecules have been illustrated in space-filling mode and hydrogen atoms are omitted for clarity.

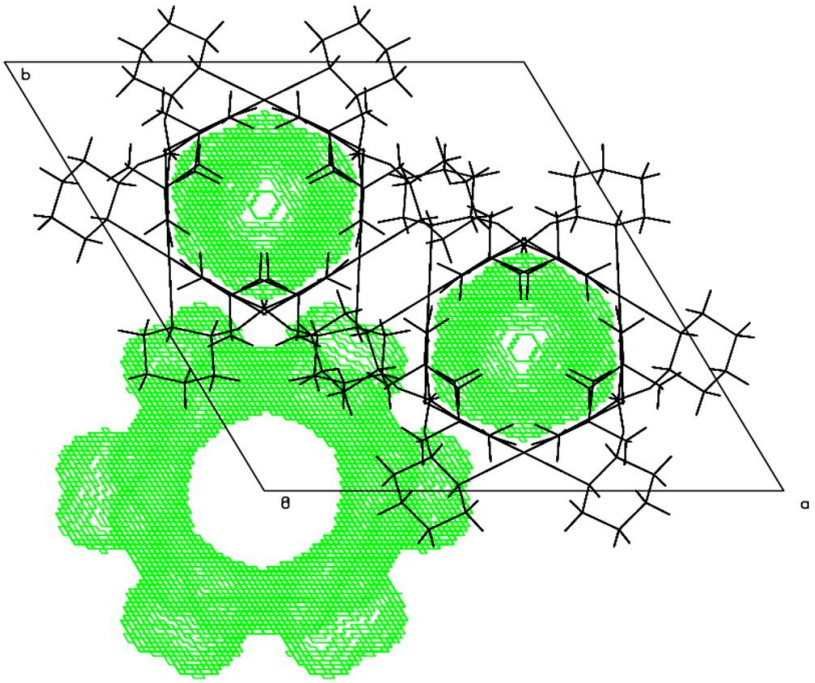

Figure S16. The areas in green represents the void from which the guest molecules were removed as viewed along *c* lattice direction

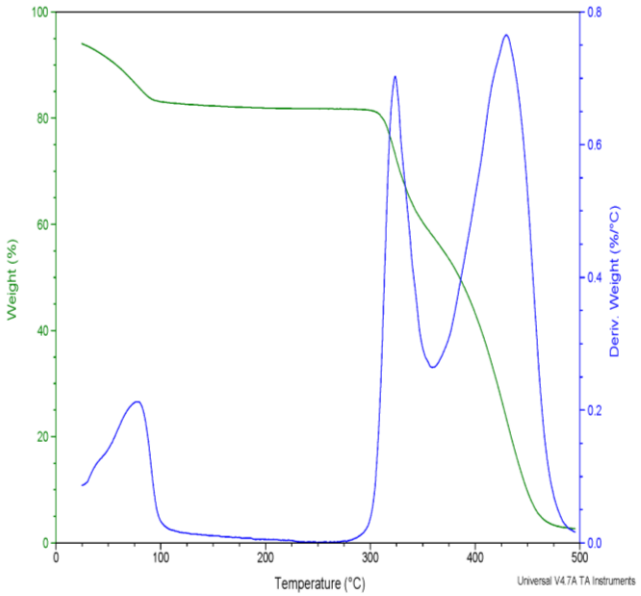

Figure S17. The TGA curve shows a 17.6% weight loss in the range of 25 to 100°C which is comparable to a loss of six molecules of methanol.

Subsequently, the remaining crystals were exposed to supercritical CO_2 for two days. After this time the single crystal X-ray diffraction experiment was carried out on one of their crystals at low temperature.

Crystal data for 3f$_{sCO2}$: $C_{54}H_{72}N_6O_3$, M_r=853.18, yellow block, 0.55×0.35×0.25 mm^3, hexagonal, space group $P6_322$ (No. 182), a=b=18.640(3), c=22.083(3) Å, V=6644.8(13) Å^3, Z=4, D_c=0.853 g/cm^3, F_{000}=1848, Bruker Quasar APEX DUO, MoKα radiation, λ=0.71073 Å, T=100(2)K, 2θ_{max}=50.8°, 34249 reflections collected, 4090 unique (R_{int}=0.0631). Final *GooF*=1.058, *R1*=0.0510, *wR2*=0.1206, *R* indices based on 3218 reflections with I>2sigma(I) (refinement on F^2), 193 parameters, 0 restraints. Lp and absorption corrections applied, μ=0.053 mm^{-1}. Absolute structure parameter=1.8(19) (Flack, H. D. *Acta Cryst*. **1983**, *A39*, 876-881).

Similarly to **3f**, the solvent molecules in crystal structure of **3f$_{sCO2}$** are highly disordered and could not be properly modelled. Therefore their contributions were removed from the diffraction data using SQUEEZE. Interestingly, the estimated electron count of 129 ē (per void vol. of 2210.6 Å^3) is much lower than that calculated for **3f** and it indicates that CO_2 may have replaced methanol. Furthermore, the crystals are less stable in air than their initial counterparts and more easily loses their crystallinity. TGA experiment performed after supercritical CO_2 exchange shows only 1.6% weight loss (Figure S20).

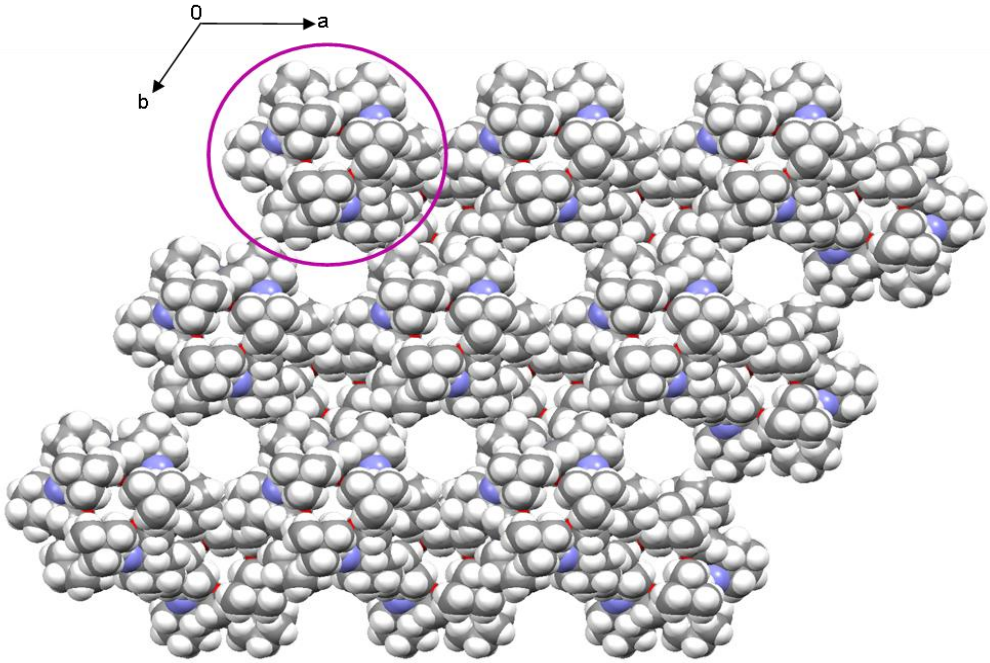

Figure S18. The host matrix in the crystals of **3f$_{sCO2}$** viewed along [001] shows two types of channels: narrow and wide, both able to accommodate solvent molecules. The narrow channels passes through the capsules (interior channels along 3-fold axis) while the wide channels are formed in the intramolecular space (exterior channels along 6_3 screw axis). Host molecules are shown in van der Waals representation. The capsule in the top view has been marked in purple cycle.

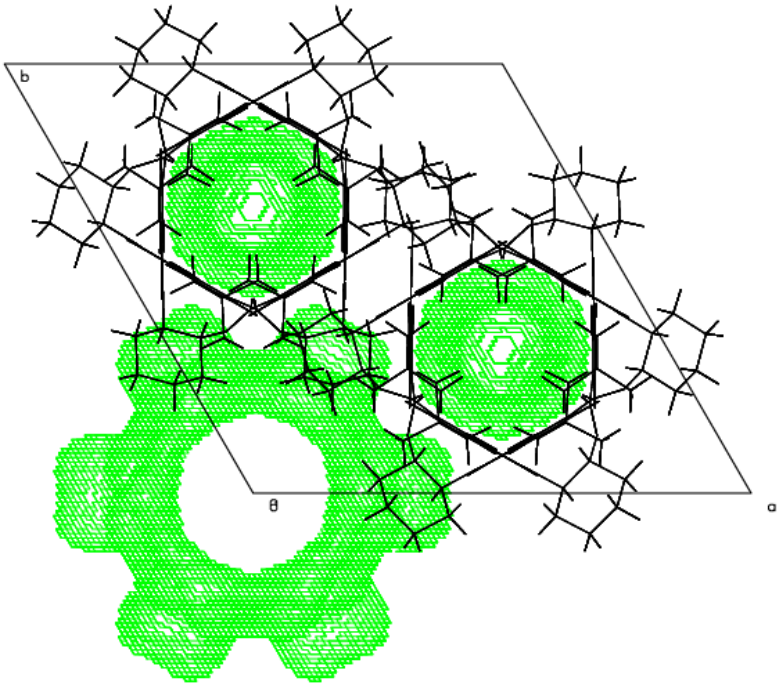

Figure S19. The areas in green represents the void from which the guest molecules were removed as viewed along *c* lattice direction.

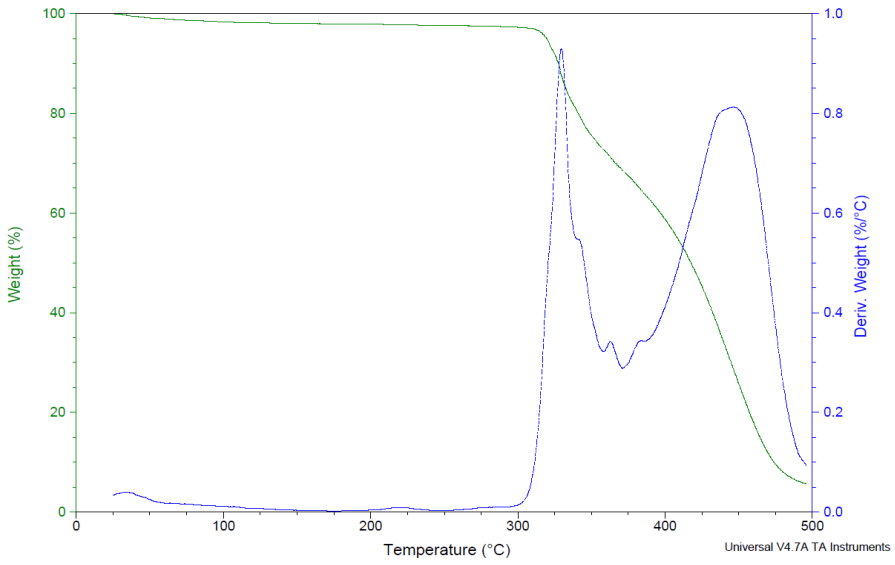

Figure S20. The TGA curve shows 1.6% weight loss in the range of 25 to 100°C.

Crystal data for 3g: $C_{99}H_{90}N_6O_3 \cdot 4(CH_2Cl_2) \cdot CH_3OH$, *Mr*=1783.52, yellow plate, 0.60×0.20×0.04 mm^3, orthorhombic, space group $P2_12_12_1$ (No. 19), *a*=14.177(2), *b*=21.094(3), *c*=32.557(4) Å, *V*=9736(2) $Å^3$, *Z*=4, D_c=1.217 g/cm^3, F_{000}=3744, SuperNova, Atlas detector, CuKα radiation, λ=1.54187 Å,*T*=130(2)K, $2\theta_{max}$=133.2°, 51554 reflections collected, 17185 unique (R_{int}=0.0410). Final *GooF*=1.046, *R1*=0.0582, *wR2*=0.1704, *R* indices based on 15826 reflections with I>2sigma(I) (refinement on F^2), 1120 parameters, 3 restraints. Lp and absorption corrections applied, μ=2.530 mm^{-1}. Absolute structure parameter=0.060(12) (Flack, H. D. *Acta Cryst*. **1983**, *A39*, 876-881).

The asymmetric unit contains one molecule of **3g**, one molecule of methanol and five molecules of dichloromethane. Since one of the five molecules of dichloromethane was highly disordered it could not be modelled properly; therefore its contribution was removed from the diffraction data using SQUEEZE. The estimated electron count is 205 in an accessible void volume of 639.9 $Å^3$ and is correlated with approximately 4 molecules of dichloromethane per unit cell. Consequently it gives one molecule of guest per void. Taking into account the squeezed molecule and solvent molecules that could be modelled, we established the ratio of host to guests as 1:5:1.

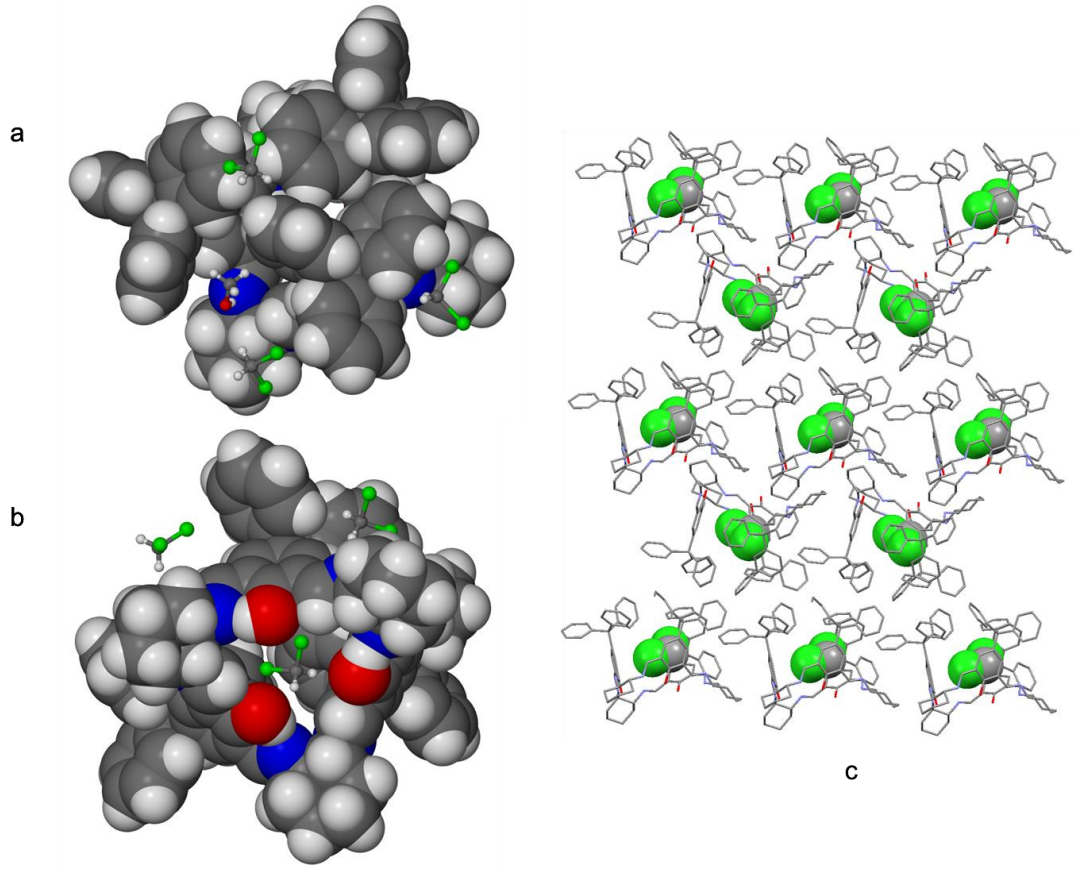

Figure S21. The top (a) and bottom (b) views of **3g** shown in van der Waals representation while solvents molecules have been illustrated in ball and stick mode. The top view demonstrates that the trityl groups completely block the entrance to the inner cavity from upper rim side and the guest molecules pack themselves in the niches formed by the bulky substituents. The bottom view shows that the inside of the macrocycle one guest molecule has been included. (c) A packing diagram of the host together with the guest molecules in the cavity of each molecular cage. All H atoms are omitted for clarity.

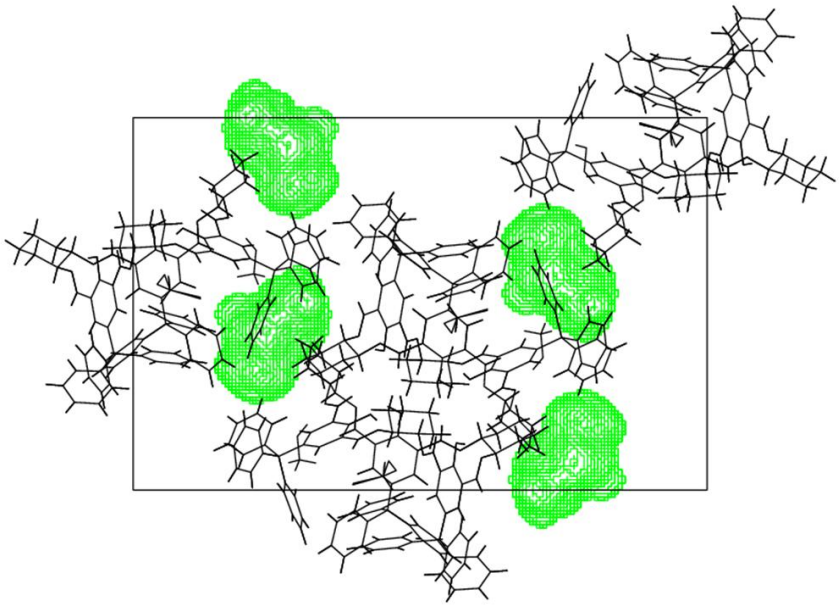

Figure S22. The areas in green represents the voids from which the guest molecules were removed as viewed along *a* lattice direction.

***Crystal data for 3g$_{MeCN}$*:** $C_{99}H_{90}N_6O_3 \cdot 0.75(C_2H_3N)$, M_r=1442.56, pale yellow plate, 0.40 x 0.20 x 0.05 mm^3, orthorhombic, space group $P2_12_12_1$ (No. 19), a=15.1450(4), b=21.4200(4), c=25.2160(6) Å, V=8180.2(3) $Å^3$, Z=4, D_c=1.171 g/cm^3, F_{000}=3066, Bruker Quasar APEX DUO, λ=1.54178 Å, T=100(2)K, $2\vartheta_{max}$=133.2°, 57004 reflections collected, 13961 unique (R_{int}=0.0642). Final *GooF*=1.034, *R1*=0.0542, *wR2*=0.1304, *R* indices based on 10601 reflections with I>2sigma(I) (refinement on F^2), 1005 parameters, 0 restraints. Lp and absorption corrections applied, μ=0.546 mm^{-1}. Absolute structure parameter=0.1(3) (Flack, H. D. *Acta Cryst*. **1983**, *A39*, 876-881).

The occupancy of the guest molecule – acetonitrile - has been refined to 0.75, hence the host: guest ratio is 3:4.

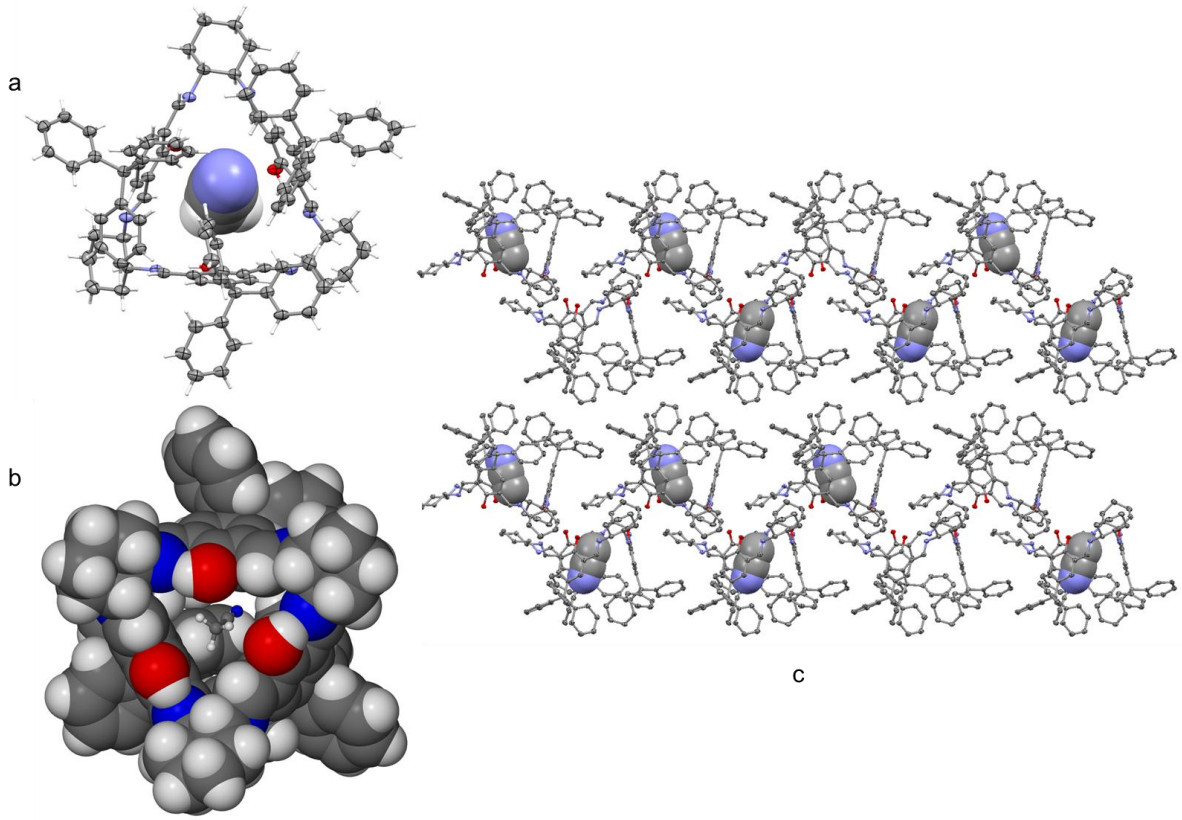

Figure S23. The top (a) and bottom (b) views of **3g$_{MeCN}$.** In (a), the host molecule is shown in ellipsoids style while the acetonitrile molecule is shown as van der Waals representation. In (b) the solvents molecules are illustrated in ball and stick style. (b) The packing diagram showing both host and guest viewed along the *c* lattice direction. Statistically the guest occupies 2/3 of all accessible cavities. All H atoms are omitted for clarity.

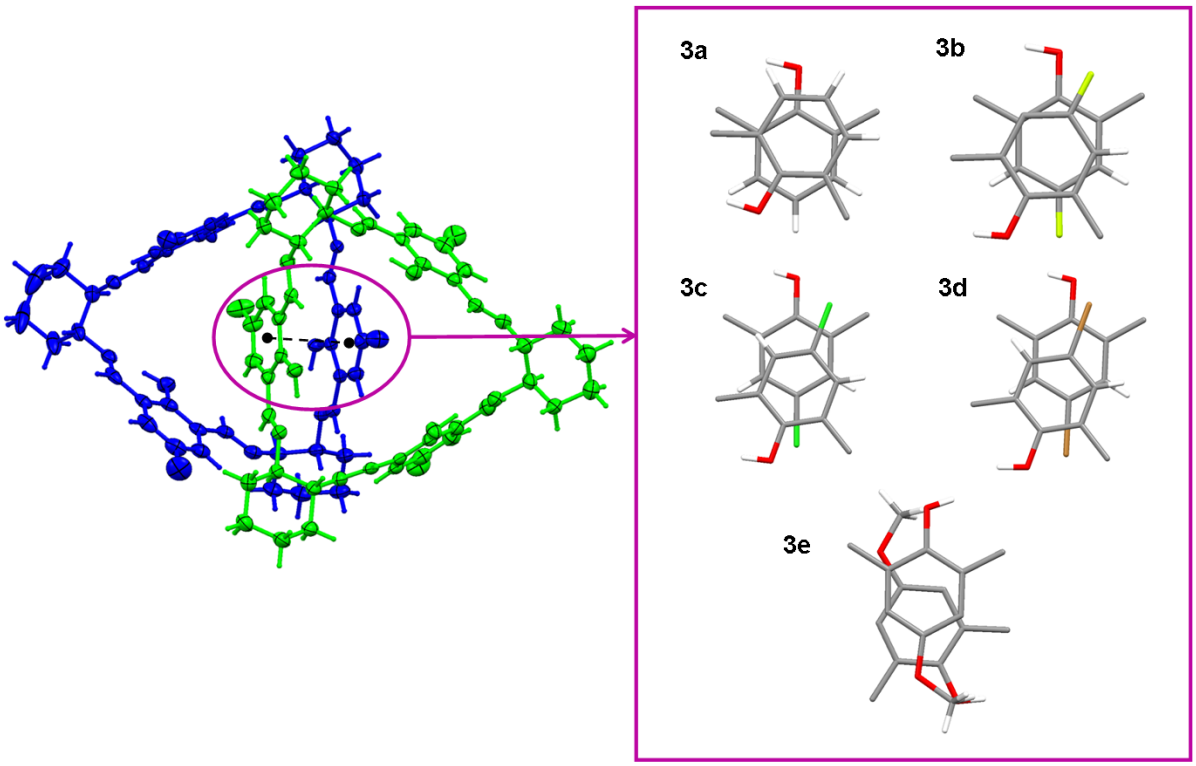

Figure S23. π…π interactions within the dimer (on the left) and overlapping mode of two phenyl rings engaged in these interactions shown as projection onto the plane of one of the ring (on the right).

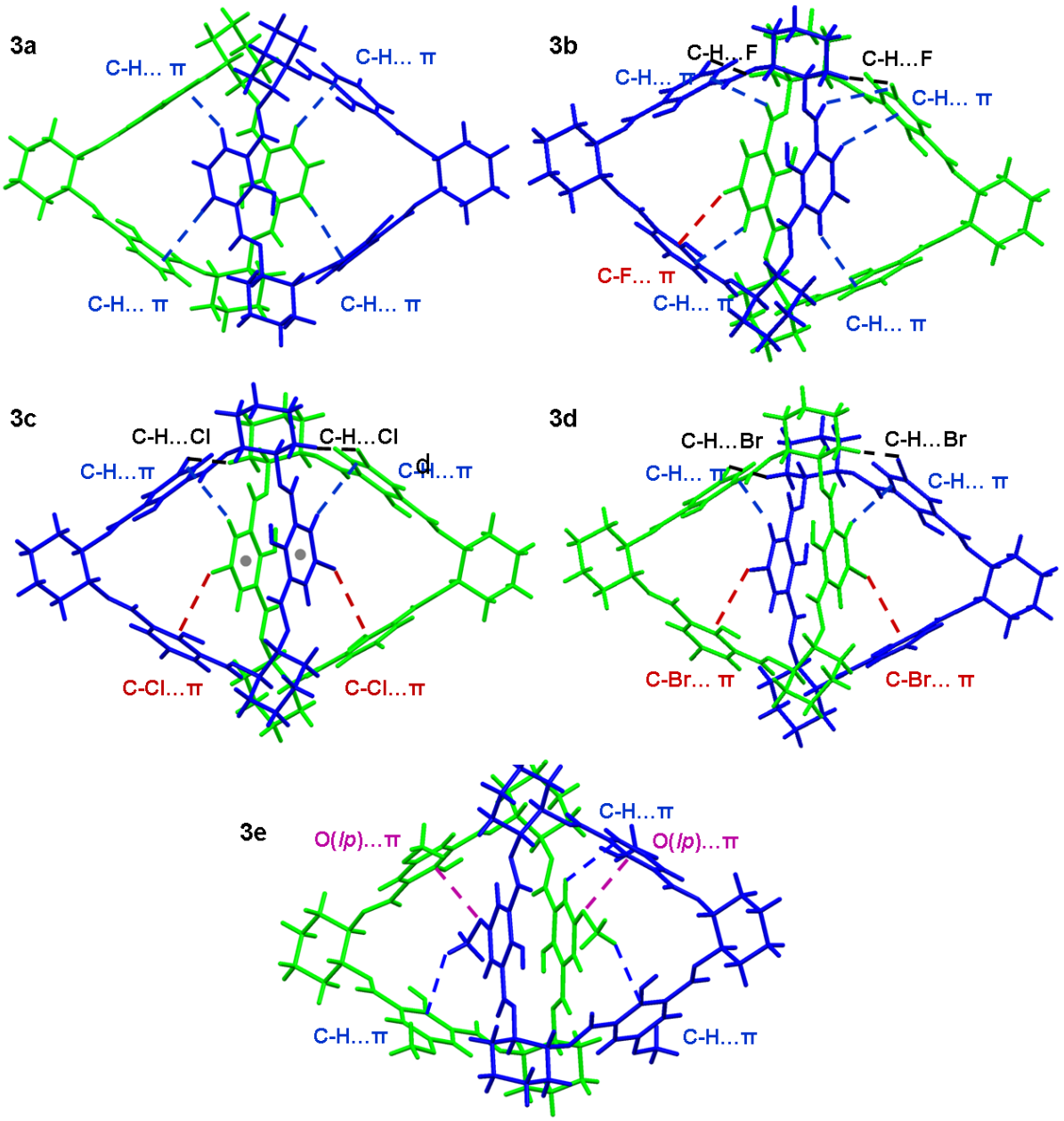

Figure S24. An illustration of weak interactions within the dimmers.

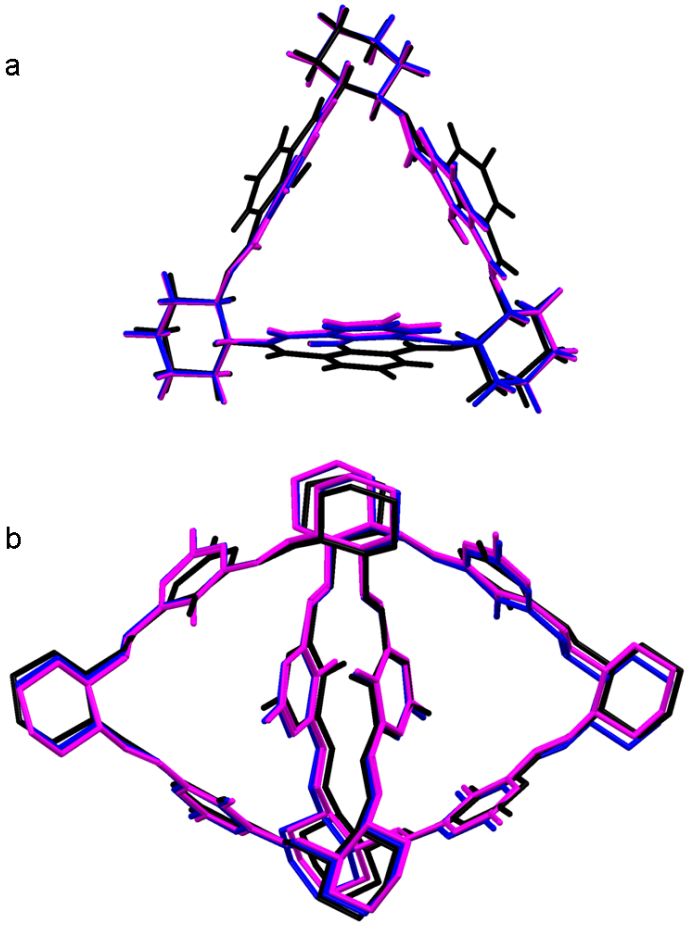

Figure S25. An overlay of the molecules (a) and dimers (b) of **3b** obtained from the crystal structure (black), the gas phase (blue) and solution phase (magenta) calculations

Table S1. Geometrical parameters describing $\pi\ldots\pi$ interactions[25] within the dimers of calixsalens **3a**-**3e** obtained from the crystals and calculated at the M06L/6-311G(d,p) level in the gas phase (g) as well as in the dichloromethane solution (s)

	h [a] [Å]			l [b] [Å]			r [c] [Å]			ϑ [d] [°]			φ [e] [°]		
	X-ray	Calcd (g)	Calcd (s)	X-ray	Calcd (g)	Calcd (s)	X-ray	Calcd (g)	Calcd (s)	X-ray	Calcd (g)	Calcd (s)	X-ray	Calcd (g)	Calcd (s)
3a	3.344(8)	3.283	3.332	3.417(8)	3.396	3.423	0.70(3)	0.87	0.78	2.1(4)	6.8	7.78	147.6(6)	144.5	144.5
3b	3.392(3)	3.294	3.301	3.419(3)	3.333	3.330	0.43(1)	0.51	0.44	0.6(2)	4.5	4.2	145.5(3)	140.7	140.9
3c	3.392(4)	3.252	3.268	3.563(4)	3.446	3.470	1.09(1)	1.14	1.17	0.6(2)	8.5	4.1	151.2(3)	160.8	153.4
3d	3.406(3)	3.373	3.272	3.740(3)	3.460	3.465	1.54(1)	0.77	1.14	0.8(2)	5.4	5.80	153.1(3)	160.9	160.9
3e	3.363(3)	3.345	3.335	3.536(3)	3.435	3.542	1.09(1)	0.78	1.19	6.2(1)	14.6	18.1	142.0(2)	151.0	158.6

[a] The mean distance between two planes of aromatic rings. [b] The centroid-centroid distance. [c] The offset of interacting rings. [d] The dihedral angle between two planes of interacting rings. [e] Twist angle, calculated as $O_{hydroxyl}$-C_{sp2}…C_{sp2}-$O_{hydroxyl}$ *pseudo*-torsion angle.

Table S2. The donor-acceptor distances (Å) for intramolecular O-H…N hydrogen bonds found in the crystals of **3a**-**3e** and their counterparts calculated for monomers and dimers at the M06L/6-311G(d,p) level.

	Crystal	Calculated monomer (gas)	Calculated monomer (solv.)	Calculated dimer (gas)	Calculated dimer (solv.)
3a					
O1…N2	2.584(7)	2.625[a]	2.611	2.640[b]	2.603[b]
O2…N4	2.589(7)		2.614	2.630	2.629
O3…N6	2.582(7)		2.613	2.613	2.618
O4…N12	2.594(6)				
O5…N14	2.587(7)				
O6…N16	2.637(7)				
3b					
O1…N2	2.603(3)	2.625[a]	2.616	2.640	2.626[b]

O2…N4	2.616(3)		2.616	2.633	2.621
O3…N6	2.599(3)		2.616	2.616	2.607
O11…N13	2.592(3)			2.640	
O12…N15	2.565(3)			2.633	
O13…N11	2.582(3)			2.616	
3c					
O1…N3	2.618(3)	2.624[a]	2.611	2.624	2.617
O2…N5	2.600(3)		2.619	2.626	2.617
O3…N1	2.606(3)		2.622	2.627	2.600
O11…N12	2.606(3)			2.626	2.617
O12…N14	2.575(3)			2.627	2.617
O13…N16	2.570(3)			2.624	2.600
3d					
O1…N2	2.611(3)	2.622[a]	2.622	2.616	2.635
O2…N4	2.587(3)		2.610	2.631	2.612
O3…N6	2.583(3)		2.628	2.624	2.609
O4…N12	2.610(3)			2.623	2.615
O5…N14	2.617(3)			2.616	2.605
O6…N16	2.611(3)			2.643	2.622
3e					
O1…N2	2.575(2)	2.632[a]	2.625	2.641	2.609
O2…N4	2.571(2)		2.626	2.632	2.612
O3…N6	2.583(2)		2.627	2.623	2.624
O4…N13	2.578(2)			2.641	2.609
O5…N15	2.556(2)			2.632	2.612
O6…N11	2.578(2)			2.623	2.624

[a] C_3 symmetry; [b] C_2 symmetry

Table S3. The donor-acceptor distances (Å) for the O-H…N hydrogen bonding in the crystals of **3f** and **3e**.

	Distance [Å]
3f	
O1…N2	2.577(2)
$3f_{sCO2}$	
O1…N1	2.567(2)
3g	
O1…N2	2.565(4)
O2…N4	2.575(4)
O3…N6	2.600(4)
$3g_{MeCN}$	
O1…N3	2.523(4)
O2…N2	2.609(4)
O3…N5	2.620(4)

References

1 C. Zondervan, E. K. van den Beuken, H. Kooijman, A. L. Spek, B. L. Feringa, *Tetrahedron Lett*., 1997, **38**, 3111.

2 W. Huang, S. Gou, D. Hu, Q. Meng, *Synt. Commun*., 2000, **30**, 1555.

3 L. F. Lindoy, G. V. Meehan, N. Svenstrup, *Synthesis*, 1998; **7**, 1029.

4 M. W. Schneider, I. M. Oppel, H Ott, L. G. Lechner, H.-J. S. Hauswald, R. Stoll, M. Mastalerz, *Chem. Eur. J*., 2012, **18**, 836.

5 K. Tanaka, R. Shimoura, M. R. Caira, *Tetrahedron Lett*., 2010, **51**, 449.

6 Z. Chu, W. Huang, L. Wang, S. Gou, *Polyhedron*, 2008, **27**, 1079.

7 K. Tanaka, T. Tsuchitani, N. Fukuda, A. Masumoto, R. Arakawa, Tetrahedron: Asym., 2012, **23**, 205.

8 D. Jacquemin, E. A. Perpète, I. Ciofini, C. Adamo, R. Valero, Y. Zhao, D. G. Truhlar, *J. Chem. Theor.*, 2010, **6**, 2071.

9 G. Scalmani, M. J. Frisch, *J. Chem. Phys*., 2010, **132**, 114110.

10 M. Kwit, J. Gawronski, D. R. Boyd, N. D. Sharma, M. Kaik, *Org. Biomol. Chem*., 2010, **8**, 5635 and literature cited therein.

11 L. Goerigk, S. Grimme, *J. Phys. Chem. A*, 2009, **113**, 767.

12 a) C. Adamo, V. Barone, *J. Chem. Phys*., 1999, **110**, 6158; b) Y. Tawada, T. Tsuneda, S. Yanagisawa, T. Yanai, K. Hirao, *J. Chem. Phys*. 2004, **120**, 8425.

13 T. Yanai, D. Tew, N. Handy, *Chem. Phys. Lett*., 2004, **393**, 51.

14 N. Harada, P. Stephens, *Chirality*, 2010, **22**, 229.

15 Gaussian 09, Revision D.01, M. J. Frisch, G. W. Trucks, H. B. Schlegel, G. E. Scuseria, M. A. Robb, J. R. Cheeseman, G. Scalmani, V. Barone, B. Mennucci, G. A. Petersson, H. Nakatsuji, M. Caricato, X. Li, H. P. Hratchian, A. F. Izmaylov, J. Bloino, G. Zheng, J. L. Sonnenberg, M. Hada, M. Ehara, K. Toyota, R. Fukuda, J. Hasegawa, M. Ishida, T. Nakajima, Y. Honda, O. Kitao, H. Nakai, T. Vreven, J. A. Montgomery, Jr., J. E. Peralta, F. Ogliaro, M. Bearpark, J. J. Heyd, E. Brothers, K. N. Kudin, V. N. Staroverov, R. Kobayashi, J. Normand, K. Raghavachari, A. Rendell, J. C. Burant, S. S. Iyengar, J. Tomasi, M. Cossi, N. Rega, J. M. Millam, M. Klene, J. E. Knox, J. B. Cross, V. Bakken, C. Adamo, J. Jaramillo, R. Gomperts, R. E. Stratmann, O. Yazyev, A. J. Austin, R. Cammi, C. Pomelli, J. W. Ochterski, R. L. Martin, K. Morokuma, V. G. Zakrzewski, G. A. Voth, P. Salvador, J. J. Dannenberg, S. Dapprich, A. D. Daniels, Ö. Farkas, J. B. Foresman, J. V. Ortiz, J. Cioslowski, D. J. Fox, Gaussian, Inc., Wallingford CT, 2009.

16 SAINT, Data Reduction Software, version 6.45, Bruker Analytical X-ray Systems Inc., Madison, WI, USA, 2003.

17 SADABS, version 2.05, Bruker Analytical X-ray Systems Inc., Madison, WI, USA, 2002.

18 CrysAlisPro, version. 1.171.35.4, Agilent Technologies, Ltd, Yarnton, England, 2010.

19 G. M. Sheldrick, *Acta Cryst. A*, 2008, **64**, 112.

20 H. D. Flack, G. Bernardinelli, *J. Appl. Cryst*. 2000, **33**, 1143.

21 L. J. Barbour, *J. Supramol. Chem*., 2001, **1**, 189.

22 POV-Ray™ for Windows, version 3.6, Persistence of Vision Raytracer Pty Ltd, Williamstown, Australia, 2004, http://www.povray.org

23 I. J. Bruno, J. C. Cole, P. R. Edgington, M. Kessler, C. F. Macrae, P. McCabe, J. Pearson, R. Taylor, *Acta Cryst. B*, 2002, **58**, 389.

24 T. L. Spek, *Acta Cryst. A*, 1990, **46**, 194.

25 U. Rychlewska, A. Plutecka, M. Hoffmann, P. Skowronek, K. Gawronska, J. Gawronski. *Acta Cryst. B*, 2009, **65**, 86.